IEEE Access
Multidisciplinary | Rapid Review | Open Access Journal

Received November 16, 2018, accepted December 16, 2018, date of publication January 1, 2019,
date of current version January 16, 2019.

Digital Object Identifier 10.1109/ACCESS.2018.2889462

Effects of Lateral Conductivity Variations on Geomagnetically Induced Currents: H-Polarization

CHUNMING LIU, XUAN WANG, SHUMING ZHANG, AND CHUNZE XIE
School of Electrical and Electronic Engineering, North China Electric Power University, Beijing 102206, China

Corresponding authors: Chunming Liu (cm_liu@163.com) and Xuan Wang (x_wang@ncepu.edu.cn)

This work was supported in part by the National Key Research and Development Plan under Grant 2016YFC0800103, in part by the National Natural Science Foundation of China under Grant 51677068, and in part by the Fundamental Research Funds for the Central Universities under Grant 2018QN007.

ABSTRACT H-polarization, along with E-polarization, indicates the lateral variations of the Earth conductivity, which influence the induced electric field distribution. The coast effect is a typical H-polarization phenomenon that causes local geoelectric field enhancement in coastal areas and significantly affects the geomagnetically induced currents (GIC) distributions in power grids. The influences of H-polarization on geoelectric fields and GIC form the basis for further research on power grid disasters resulting from magnetic storms. In this paper, block and thin-shell models of the coast effect are established, and the electric field distribution in the case of H-polarization is calculated using the finite element method. The results demonstrate the effects of the conductivity, frequency, and distance from the interface of a different conductivity on electric field distortion. Additionally, the relationship between H-polarization and GIC in power grids is investigated, demonstrating that the GIC can be influenced within 100 km in the H-polarization case. The methods and results provide a theoretical basis for GIC risk assessment and development of a control strategy for the power grid.

INDEX TERMS Finite element method (FEM), geomagnetically induced currents (GIC), coast effect.

I. INTRODUCTION

The geoelectric field induced in the ground by spatiotemporally varying magnetosphere - ionosphere electric current system drives geomagnetically induced currents (GIC) in artificial conductors. These GIC disrupt the normal operation of power grids, high-speed railways, and oil and gas pipelines [1]–[3]. In areas with complex geological structures, such as coasts and plate boundaries, the Earth conductivity varies significantly. Owing to the lateral variations of the Earth conductivity, the induced geoelectric field will be distorted and the ground potential will change sharply. It is called ''H-polarization'' the case when the geomagnetic field horizontal component is perpendicular to the conductivity gradient, i.e. parallel to the interface of conductivity variation [4]. The phenomenon H-polarization of the geoelectric field is illustrated in Fig. 1.

The coast effect [5], which is a typical H-polarization phenomenon, refers to the conductivity of seawater to be significantly greater than that of the adjacent land [6]. During geomagnetic disturbances (GMD), the induced current density through the land–sea boundary must be continuous with the charges accumulation at the boundary. That increases the electric field in the low-conductivity land side and enlarges the GIC in power grids located at coastal areas while decreases the electric field in the high-conductivity sea side [7], [8].

Previously Simpson and Bahr [9] first went into detail on practical aspects of applying the Magnetotelluric (MT) technique, which is a technique for probing the electrical conductivity structure of the Earth to depths of up to 600 km. Berdichevsky and Dmitriev [10] considered a model of the inhomogeneous Earth with plane-wave primary field. They also presented a set of basic two-dimensional (2-D) and three-dimensional (3-D) models to study the near-surface magnetotelluric anomalies caused by geoelectric inhomogeneities in the sediments and deep geoelectric inhomogeneities located in the consolidated Earth's crust and the upper mantle. The numerical methods and boundary conditions outlined in this chapter [11] aimed to capture such geological complexity and replicate its electromagnetic response through discretized

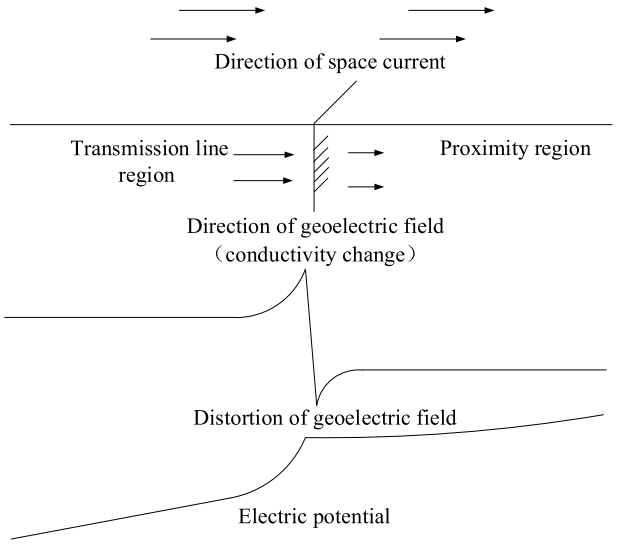

FIGURE 1. H-polarization of an electric field.

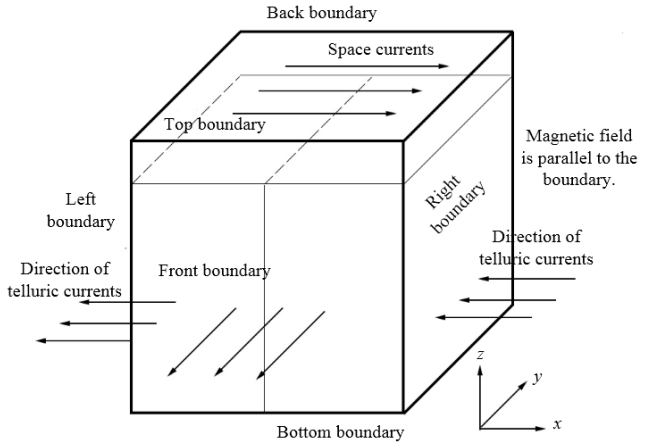

FIGURE 2. Geoelectric field model of H-polarization.

numerical methods for solving the governing equations. These above-mentioned books definitely provided the basic principles of electromagnetic induction in the Earth and methods for modeling the complex geoelectric structures, which laid important foundations for the work of this paper.

The coast effect has also been discussed in previous literature. For instance, Gilbert modeled the electric field distribution near an ocean–land interface by using a two-region model and demonstrated that the coast effect can significantly impact the GIC in the power grid [12]. Another study showed that the local geoelectric field enhancement resulting from the abrupt lateral conductivity change between sea water and land can be more than 10 V/km, which is significantly greater than the electric field strength of 1 V/km that is typically associated with an induced electric field [13]. Boteler explained the cause of the coast effect as the difference between the current densities from the high-conductivity inflowing interface and the interface flowing into the low-conductivity area [14], when the telluric currents are perpendicular to the interface.

These studies confirmed that the Earth conductivity structure is one of the main factors impacting the magnitudes of geoelectric fields and preliminarily revealed the coast effect mechanism. However, there is no quantitative description of the correlation between the lateral conductivity variations of the Earth and geoelectric field distortion.

The main objectives of this research are to assess the influences of H-polarization on the geoelectric field intensity and GIC. To realize these objectives, we present a 2-D finite element analysis about the influence of lateral variations in the Earth conductivity on the electric field, which is induced in the Earth by the geomagnetic field variations caused by space weather-related currents in the ionosphere. We develop block and thin-shell models for electric field distribution simulation. The numerical results quantify the H-Polarization in terms of the variation in the magnitude of E-field as a function of the ratio of the low and high conductivities, frequency, and also estimate how far from the boundary the H-Polarization extends. We then evaluate the influence of the geographical electric field distribution on the GIC in power grids and conclude that with lateral Earth conductivity variations, the influences of E- and H-polarization on geoelectric fields should be considered comprehensively. Our results provide a theoretical basis for GIC evaluation in areas with complex geological structures and enable us to put forward some suggestions for ultra-high-voltage power grid disaster prevention in the next solar cycle.

II. MODEL AND METHODS

A. GEOELECTRIC FIELD AND CURRENT SOURCE MODEL

For H-polarization, a 3-D block model with lateral conductivity variations is established for geoelectric field simulation, as shown in Fig. 2. In the Cartesian coordinate system, x points to the direction of conductivity change, y points to the direction of the horizontal extension of the discontinuity, and z points upwards. The Earth conductivity model consists of two regions with constant conductivities. The interface of the sudden change is set at $x = 0$, which could represent a coastline, plate boundary, or rock fracture surface. The transmission line is located in the region with $x < 0$, and the area with $x > 0$ is called the "proximity region."

The space currents are assumed to span both the "transmission line region" and the "proximity region". The surface current density is set to 1 A/m, changing sinusoidally over time. The current source is located a height of 100 km above the surface of the Earth. The current direction is set parallel to the positive x-axis. The hypothetical conditions are the same as those used in the E-polarization investigation: the electric field is produced only by the magnetic field variations, irrespective of the electric field produced by stationary charges in the Earth; all of the magnetic permeability values in the solution domain are equal to the vacuum permeability, $\mu_0 = 4\pi \times 10^{-7}$ H/m; the Earth conductor is isotropic and the conductivity does not change with time; the conductivity of

each structure does not vary spatially; and abrupt conductivity variations occur only at the interfaces between different structures. The finite element method (FEM) suitable for solving 2-D or 3-D problems by using the Galerkin method of weighted residuals [15] is employed to model the lateral variations of the Earth conductivity structure.

B. BOUNDARY PROBLEM SIMPLIFICATION

The boundary conditions are simplified in the same way as in the E-polarization case. For H-polarization, the surrounding boundary conditions need to be noted. The telluric currents induced by space currents flow vertically into the left and right boundary surfaces, yielding the boundary condition

$$A_y = A_z. \tag{1}$$

Meanwhile, the telluric currents are parallel to the front and back boundary surfaces. Accordingly,

$$\boldsymbol{e}_y \times \left(\frac{1}{\mu_0}\nabla \times \boldsymbol{A}\right) = 0. \tag{2}$$

where $\boldsymbol{A}$ expresses vector potential, A_y and A_z are respectively the y component and z component of $\boldsymbol{A}$, e_y is the normal unit vector of the front boundary, which points in the positive y-direction, the permeabilities of air and the Earth are both assumed to be μ_0.

III. SIMPLIFIED MODEL OF THE EARTH CONDUCTIVITY STRUCTURES

A. SIMPLIFIED BLOCK MODEL AND THIN SHELL MODEL

The space current is defined as being perpendicular to the interface i.e. parallel to the x axis, and all of the field quantities are invariant in the y-direction. According to the shape of the space current source, the magnetic field has both y- and z-components, while the magnetic vector potential has only an x-component. Through parameter transformation, the problem can be treated as a 2-D field problem in the x–z plane, which is shown in Fig. 3. At this point, since the conductivity varies in the same direction as the electric field intensity, the electric field intensity and induced current have both x- and z- components. A coefficient k describes the Earth conductivity variations, which is the ratio of conductivity in the proximity region and transmission line region. The transmission line is located in the basic conductivity region where $x < 0$ and the conductivity is set to 0.01 S/m, which is commonly seen in rocks containing slight amounts of water [16]. The conductivity in the proximity region $x > 0$ is set to $0.01k$ S/m.

This block model is too simple to be applicable to coastal areas. Lateral conductivity variations usually arise at shallow depths below the surface of the Earth, such as along coasts, in lakes, and in sedimentary plains. When the thickness and frequency are both constant, the geoelectric field is mainly affected by the surface conductivity. Therefore, studies on the quantitative relation between surface conductivity and geoelectric field variations are of great importance for illustrating the influence of the earth conductivity structure on GIC in

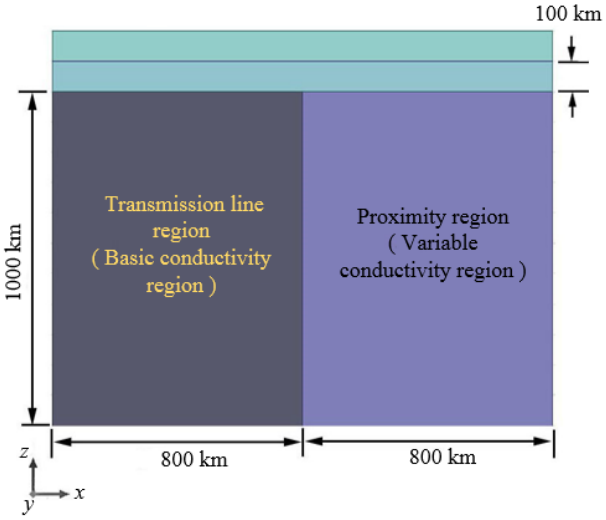

FIGURE 3. Simplified block model with two parts.

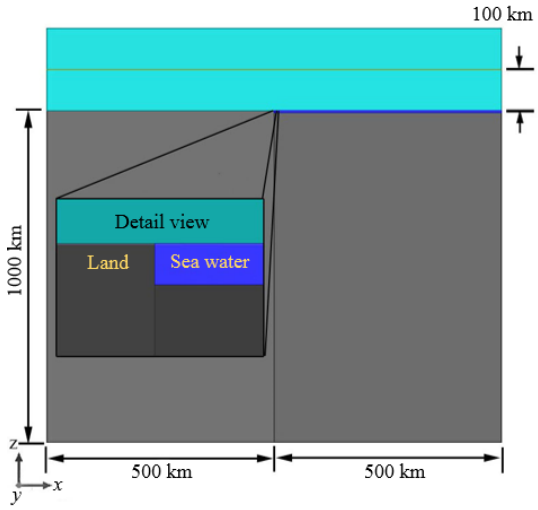

FIGURE 4. Simplified thin shell model.

power grids. Thus, a thin shell model is also established in this study, as shown in Fig. 4 with a typical conductivity distribution in a coastal area.

The term ''coast effect'' here refers to the phenomenon in which lateral surface conductivity variations cause geoelectric field distortions, so the land conductivity is assumed to be uniform. In a coastal region, the seawater conductivity is high and almost identical in different areas. The sea is set as the basic conductivity region in this study, with conductivity $\gamma = 4$ S/m. The complicated Earth conductivity structures indicate that the land conductivity differs significantly, so land is set as a variable conductivity region. In the model, the air conductivity, with $z > 0$ km, is set to 0 S/m. The basic conductivity region is in the shell region, $x > 0$ km and -5 km $< z < 0$ km, which is used to model seawater. The variable conductivity region is divided into two parts,

$x < 0$ km, $x > 0$ km and $z < -5$ km, which represent the land and seabed, respectively. The source is located at $z = 100$ km.

B. GOVERNING EQUATIONS AND BOUNDARY CONDITIONS

For H-polarization, the eddy current field is a parallel plane field along the x-axis. The magnetic vector potential has only an x-component, so it can be determined using the scalar A_x. In addition, the vector potential satisfies the Coulomb gauge equation. The governing equations can be written as

$$-\frac{1}{\mu}\left(\frac{\partial^2 A_x}{\partial z^2}+\frac{\partial^2 A_x}{\partial y^2}\right)+j\omega\gamma A_x = J_{sx} \tag{3}$$

and

$$\nabla\cdot\gamma\left(j\omega A_z+\nabla\varphi\right)=0. \tag{4}$$

In the typical FEM simulation software, the field component directly obtained using the 2-D field is A_z. To solve a problem in which the current is parallel to a plane in a 2-D field, it is necessary to convert the field parameters. We transform a complex 3-D problem into a 2-D field using the parameter transformation method [17]. In the non-source region, the basic equation can be expressed in terms of the magnetic field intensity:

$$-\frac{1}{\gamma}\left(\frac{\partial^2 H_y}{\partial z^2}+\frac{\partial^2 H_y}{\partial x^2}\right)+j\omega\mu H_y = 0. \tag{5}$$

Then, the electric field intensity can be obtained:

$$\boldsymbol{E}=\frac{1}{\gamma}\nabla\times\left(H_y\boldsymbol{e}_y\right)=\frac{1}{\gamma}\left(\frac{\partial H_y}{\partial x}\boldsymbol{e}_z-\frac{\partial H_y}{\partial z}\boldsymbol{e}_y\right). \tag{6}$$

In a quasi-static situation, the Poisson equation of the magnetic vector potential can be written as

$$-\frac{1}{\mu}\left(\frac{\partial^2 A_y}{\partial z^2}+\frac{\partial^2 A_y}{\partial x^2}\right)+j\omega\gamma A_y = 0. \tag{7}$$

The magnetic field intensity can be derived from the magnetic vector potential, and the magnetic field is perpendicular to the magnetic vector potential:

$$\boldsymbol{H}=\frac{1}{\mu}\nabla\times\left(A_y\boldsymbol{e}_y\right)=\frac{1}{\mu}\left(\frac{\partial A_y}{\partial x}\boldsymbol{e}_z-\frac{\partial A_y}{\partial z}\boldsymbol{e}_y\right). \tag{8}$$

Since (5) and (6) are similar to (7) and (8), respectively, the conductivity is assigned the actual permeability values in the simulation, and the permeability is assigned the actual conductivity values. Consequently, the magnetic vector potential represents the actual magnetic field intensity, the magnetic field intensity corresponds to the actual electric field intensity, and the magnetic flux density corresponds to the actual telluric current intensity.

The boundary conditions are as follows: the telluric currents at the front and back boundary surfaces are parallel; the magnetic field is perpendicular to the boundary surfaces; the telluric currents on the left and right sides are vertical to the boundary surfaces; and the magnetic field is parallel to the interface: $A_z = A_y = 0$. To ensure the continuity of the currents on the left and right sides, we set the scalar potentials at the left and right boundaries equal: $\varphi_{x=-800} = \varphi_{x=800}$. The electromagnetic field at the lower boundary attenuates to zero: $A_{z=-1000} = 0$. At the interface, the normal component of the current density and tangential component of the magnetic field intensity are both continuous.

C. PARAMETERS FOR H-POLARIZATION ANALYSIS

In this analysis, we set the following parameters:

E_{xc}: the reference value of the electric field intensity in the variable conductivity region;

E_{xb}: the reference value of the electric field intensity in the basic conductivity region;

E_{xmax}: the maximum value of the geoelectric field near the interface in the basic conductivity region;

E_{xmin}: the minimum value of the geoelectric field near the interface in the variable conductivity region;

E_{xmax}/E_{xb}: the maximum aberration rate;

$\Delta E_{xb} = E_{xmax} - E_{xb}$: the maximum distortion amplitude of the electric field in the basic conductivity region;

$\Delta E_{xc} = E_{xc} - E_{xmin}$: the maximum amplitude of the electric field distortion in the variable conductivity region;

$E_x(x)$: the intensity of the geoelectric field accounting for the H-polarization effect;

$\Delta E_x(x) = E_x(x)$ - E_{xb}: the amplitude variation of the electric field intensity with the H-polarization effect;

$x_{10\%}$: 10% influence range, $\Delta E_x(x_{10\%}) = 0.1\Delta E_{xb}$. An area is influenced by H-polarization when $\Delta E_x(x) > 0.1\Delta E_{xb}$.

IV. NUMERICAL RESULTS

A. ELECTRIC FIELD DISTRIBUTION IN THE BLOCK MODEL

The magnetic flux and electric field intensities at $f = 0.001$ Hz and $k = 10$ in the block model are shown in Figs. 5a and 5b, respectively, from the surface of the Earth to 500 km underground. The calculation results are as follows: $E_{xb} = 0.887$ V/km, $E_{xc} = 0.280$ V/km, $E_{xmax} = 1.117$ V/km, $E_{xmin} = 0.126$ V/km, $E_{xmax}/E_{xb} = 1.26$, $\Delta E_{xb} = 0.890$ V/km, and $\Delta E_{xc} = 0.154$ V/km.

Figs. 5 show that in the direction of the conductivity variations, the H-polarization increases the electric field intensity in the low-conductivity region and decreases that in the high-conductivity region. Modeling and calculations are performed using the 3-D block model to verify the feasibility of the method [18], [19]. The results are consistent with those of the 2-D model within acceptable error, so the 2-D model can be used to improve the calculation speed maintaining the analysis accuracy.

The factors influencing the geomagnetic field amplitude include the GMD frequency f, conductivity change, and distance from the interface. f mainly affects the reference values of the electric field on both sides of the interface and has little effect on the distortion rate, so we mainly investigate the surface electric field variations with k.

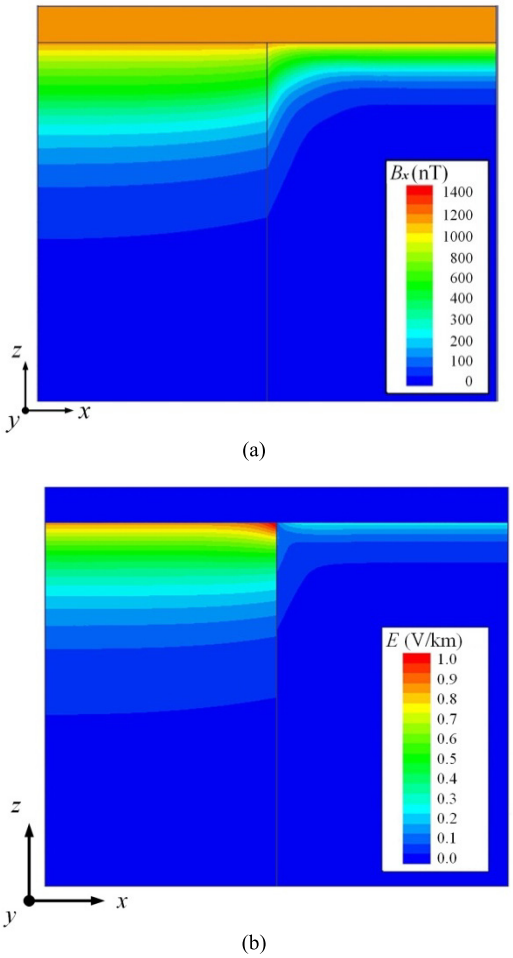

FIGURE 5. Field distributions in the block model in the case of H-polarization with $f = 0.001$ Hz and $k = 10$. (a) Magnetic field distribution. (b) Electric field distribution.

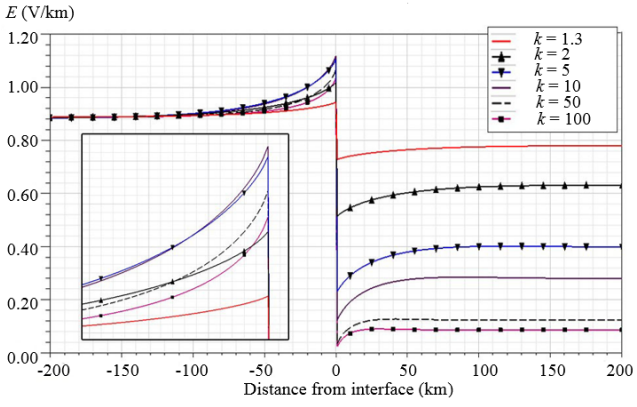

FIGURE 6. Geoelectric field distribution at the surface of the Earth with different k in the block model ($f = 0.001$ Hz).

Taking $f = 0.001$ Hz as an example, the results shown in Fig. 6 are obtained, which illustrate that the influence of H-polarization on the geoelectric field is related to k. Notably, ΔE_{xb} does not increase monotonically with k.

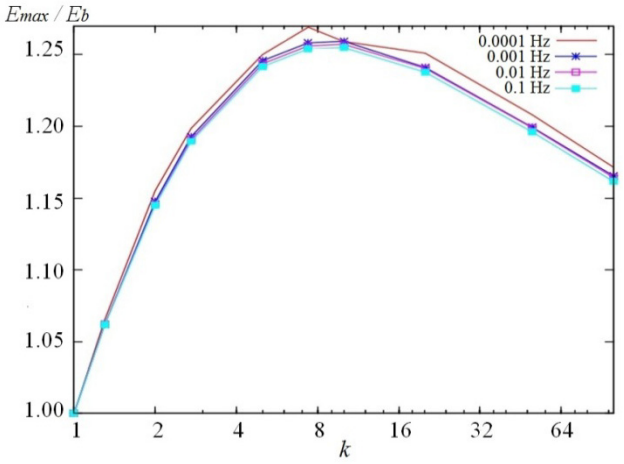

FIGURE 7. Variation of surface electric field distortion rate with k in the block model of H-polarization.

The maximum electric field distortion rate E_{xmax}/E_{xb} varies with k, as shown in Fig. 7. When $k < 10$, ΔE_{xb} is positively correlated with k. Meanwhile, it is negatively correlated with k when $k > 10$. The same results are obtained after improving the meshing accuracy near the interface. It can be inferred that there is a k in the block model at which the influence of H-polarization is maximized, which lies between 8 and 10 and can be denoted as k'.

This phenomenon can be explained in terms of telluric currents. Due to the continuity of the currents, the boundary conditions at the interface in a conductive medium are given by [20]

$$J_{bx} = J_{cx} \tag{9}$$

and

$$E_{bz} = E_{cz}. \tag{10}$$

As k varies from 1 to k', the skin depth decreases on the variable conductivity side and the telluric currents gradually tend to the surface. Meanwhile, the telluric currents in the basic conductivity region converge at the surface to ensure that the normal component of the current at the interface is continuous. Due to the accumulation of telluric currents, the vertical component of the geoelectric field near the interface increases. The surface geoelectric field increases on the low-conductivity side. Owing to the increased conductivity difference, when $k > k$', one side of the interface can be regarded as a poor conductor, while the other side is a good conductor. According to (9) and (10), the currents on the poorly conducting side tend to flow vertically into the more conductive side, and some telluric currents at the interface find other paths. This effect is dominated by k, which weakens the current collection effect in the basic conductivity region.

To determine the range of influence of H-polarization in the block model, $x_{10\%}$ is simulated with different f and k, and the results are presented in Fig. 8.

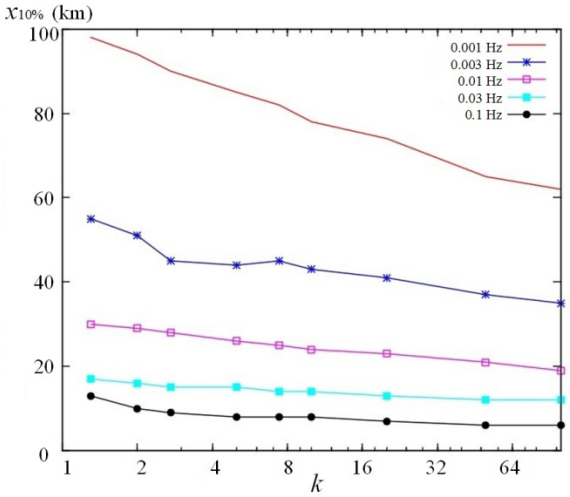

FIGURE 8. $x_{10\%}$ with different f and k of H-polarization.

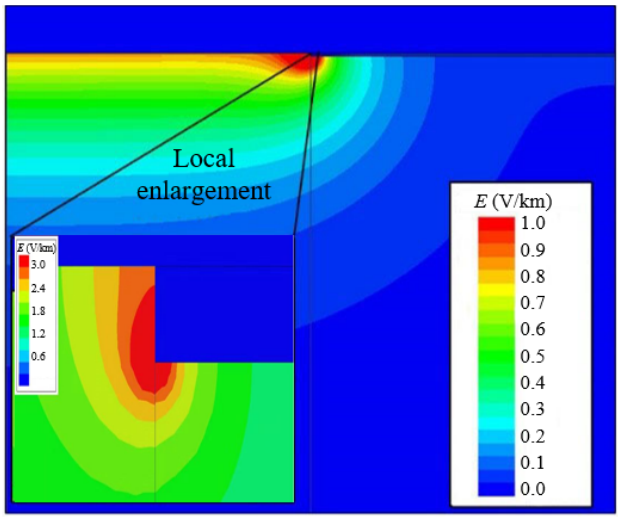

FIGURE 9. Electric field amplitude distribution in the thin shell model with H-polarization.

These results illustrate that $x_{10\%}$ is correlated with f and weakly related to k. When $f > 0.001$ Hz, the range of influence of H-polarization is less than 100 km in the block model. Using a common f value, $f = 0.01$ Hz, as an example, $x_{10\%}$ is determined to be about 20–30 km, which is far smaller than that in the case of E-polarization. Thus, if a transmission line passes through the interface within 30 km, the influence of H-polarization should be considered.

When $f = 0.001$ Hz and the conductivity difference reaches 100 times, the distortion amplitude due to H-polarization 10 km from the interface, ΔE_x (10), is 0.08 V/km, which is 9% of E_{xb} and 54.4% of ΔE_{xb}. This phenomenon differs significantly from the actual situation in coastal areas. Since the block model ignores the large vertical conductivity changes near coasts, it can only be used to simulate geoelectric field distributions in land regions with uniform conductivity and is inappropriate for complicated geological structures, such as coasts, lakes, and deposited plains. Thus, it is necessary to consider the Earth conductivity structure in the abovementioned situations.

B. ELECTRIC FIELD DISTRIBUTION IN THE THIN SHELL MODEL

In this analysis, f is 0.0001–0.1 Hz range, and γ is 0.001–2 S/m. As an example, the geoelectric field distribution from the ground surface to 500 km underground that is obtained with $f = 0.001$ Hz, $\gamma = 0.01$ S/m, and $k = 400$ is shown in Fig. 9. The calculation results obtained using the thin shell model are as follows: $E_{xb} = 0.887$ V/km, $E_{xc} = 0.045$ V/km, $E_{xmax} = 2.783$ V/km, $E_{xmin} = 0.010$ V/km, $E_{xmax}/E_{xb} = 3.14$, $\Delta E_{xb} = 1.896$ V/km, and $\Delta E_{xc} = 0.035$ V/km. The geoelectric field apparently decreases sharply at the interface between the basic and variable conductivity regions.

Since the land and sea floor have the same conductivity, the geoelectric field is continuous underground. The maximum

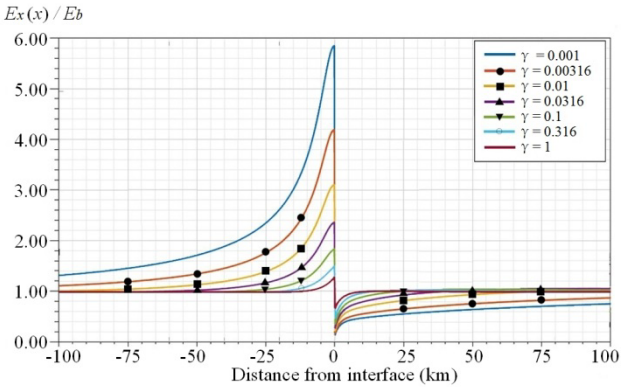

FIGURE 10. Normalized geoelectric field at the surface of the Earth in the thin shell model with $f = 0.001$ Hz and $\gamma = 0.001$–1 S/m.

geoelectric field arises at the interface between the land and sea. The distortion near the interface is clearly increased in this case compared to that obtained using the block model with $k = 400$. Next, the surface geoelectric fields with different k are calculated. The data are normalized to contrast the geoelectric fields with different conductivities. The geoelectric fields in the land and ocean regions are divided by the reference values in the corresponding regions. The normalized surface electric field obtained with $f = 0.001$ Hz is presented in Fig. 10.

The geoelectric field distortion in the thin shell model is evidently much larger than that in the block model. Moreover, unlike in the block model, when $f = 0.0001$–0.1 Hz, ΔE_{xb} decreases with increasing conductivity in the basic conductivity region. Specifically, ΔE_{xb} monotonically increases with k. The variation of the geoelectric field distortion rate with γ in the thin shell model is shown in Fig. 11.

Fig. 11 indicates that when f is low, the geoelectric field distortion rate decreases with the increasing conductivity, so the geoelectric field distortion rate increases with the

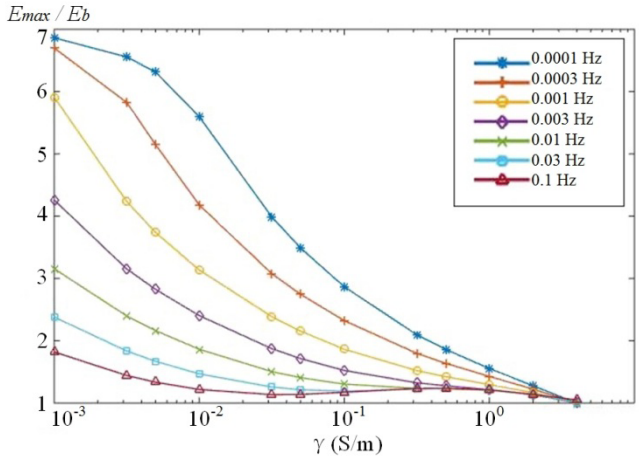

FIGURE 11. Variation of the geoelectric field distortion rate with γ when $f = 0.0001$–0.1 Hz in the thin shell model.

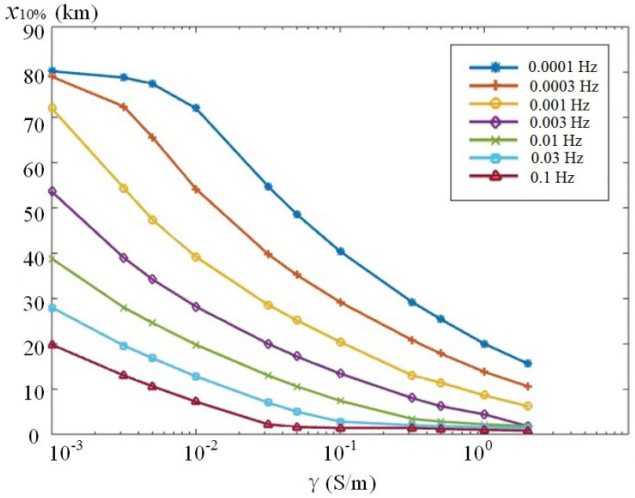

FIGURE 12. Variation of $x_{10\%}$ with γ when $f = 0.0001$–0.1 Hz in the thin shell model.

conductivity difference between the land and sea. When f is high ($f > 0.01$ Hz), the distortion rate increases and then decreases with increasing conductivity difference. This phenomenon can be explained by the flow path of the telluric currents. As f increases, the skin depth decreases and the currents in the variable conductivity region tend to flow toward the surface of the Earth. This effect increases the perpendicular component of the telluric currents as well as the electric field on the low-conductivity side. However, when the conductivity differs significantly between the two sides, the boundary conditions limit the increase of the vertical component. The area below the seabed is not affected by the vertical boundary, so the perpendicular component of the telluric currents still increases. The upward accumulation of the telluric currents causes an increase in the horizontal component of the telluric currents on the low-conductivity side, resulting in a continuous increase in the surface electric field on that side. However, when the lateral difference in conductivity increases continuously, currents tend to flow perpendicular to the interface. This effect decreases the gathering of currents to the sea, and the greater the conductivity difference is, the stronger the weakening effect is.

To determine the relationships between the range of influence of the coast effect and f and γ, $x_{10\%}$ is calculated with different f. The results are shown in Fig. 12.

When $f = 0.0001$–0.1 Hz, the influence of the coast effect extends 80 km from the interface. For example, with $\gamma = 0.01$ S/m and $f = 0.001$ Hz, $x_{10\%} = 39$ km. Therefore, when a transmission line is located within 80 km of the shoreline, it is necessary to evaluate the influence of the coast effect on the GIC.

When $f = 0.001$ Hz, $\gamma = 0.05$ S/m, and $k = 80$, the distortion amplitude at 10 km ΔE_x (10) is 0.1765 V/km, which is 44.5% of E_{xb} and 38.5% of ΔE_{xb}. Thus, the conductivity distortion in the thin shell model is much greater than that in the block model, demonstrating that the thin shell model is more suitable for environments such as coasts, lakes, and sedimentary plains. If sufficient conductivity data are available to characterize conductivity profiles of the Earth, accurate Earth conductivity models can be developed by using layered conductivity models and considering lateral variations.

C. GIC MODELING

Since the H-polarization affects the geoelectric field parallel to the conductivity gradient, we further analyze the GIC in a transmission line parallel to the conductivity gradient. We define the distances between grounding points N_1 and N_2 and the interface as x_1 and x_2, respectively, and suppose that $x_1 < x_2$. There are n computational nodes between N_1 and N_2, and the interval is Δx. Due to the phase difference, we use the real part of the electric field intensity to calculate the equivalent voltage source, which is given by

$$E_{x,i} = \mathrm{Re}\left\{E_x\left[x_1 + (i-1)\Delta x\right]\right\}, \tag{11}$$

where $E_{x,i}$ represents the real part of the x-component of the electric field intensity at node i. The equivalent voltage source between the two ground points may be represented as

$$U_{1,2} = \sum_{i=1}^{n} \frac{E_{x,i} + E_{x,i+1}}{2} \cdot \Delta x. \tag{12}$$

Then, the GIC between the two grounding points is given by

$$I_{1,2} = \frac{U_{1,2}}{R_L + R_{T1} + R_{T2}}, \tag{13}$$

where R_{L} is the line resistance, and the transformer winding and ground resistances are represented by R_{T1} andR_{T2}, respectively.

D. INFLUENCE OF COAST EFFECT ON GIC

To study the influence of the coast effect on GIC at different f and γ, we consider a 50-km-long transmission line

TABLE 1. GIC amplitudes in a power line for different f and γ. The numbers in parentheses represent GIC amplitudes without considering coast effect.

γ (S/m)	1	0.316	0.1	0.0316	0.01	0.00316	0.001
0.0001Hz	0.589 (0.561)	1.168 (0.998)	2.474 (1.774)	5.530 (3.120)	12.97 (5.52)	25.77 (9.56)	57.70 (20.60)
0.001 Hz	1.770 (1.766)	3.218 (3.149)	6.082 (5.609)	12.16 (9.983)	25.74 (17.73)	57.07 (31.10)	134.6 (55.01)
0.01 Hz	5.502 (5.507)	9.948 (9.882)	17.61 (17.66)	32.00 (31.49)	60.57 (56.09)	121.5 (99.83)	257.5 (177.4)
0.1 Hz	16.59 (16.59)	30.45 (30.45)	55.01 (55.07)	98.38 (98.82)	175.8 (176.6)	319.2 (314.9)	604.0 (560.9)

perpendicular to the shoreline with one ground terminal 5 km from the interface, $x_1 = 5$ km, $x_2 = 55$ km, $\Delta x = 0.2$ km, and $R_L + R_{T1} + R_{T2} = 2.5\Omega$. The results are shown in Table 1.

As f decreases, the impacts of the coast effect on the GIC and geoelectric field increase. When the GIC is determined based on the integral of the geoelectric field, a larger range apparently leads the GIC to increase more. The coast effect significantly influences the low-frequency component of the GIC. The GIC is positively correlated with the difference in conductivity between the land and sea when $f = 0.0001$–0.01 Hz. If f is low ($f < 0.001$ Hz) and the conductivity on the land side is very small (0.001 S/m), the coast effect makes the GIC increase 2–3 times.

In addition, when f is higher (0.1 Hz) and the land conductivity is very small (0.001 S/m), the GIC is less than that if the geoelectric field is uniform. At this point, the coast effect negatively influences the GIC. Since the surface electric field intensity near the interface has different phases at different positions, the values do not reach their maxima at the same time. The electric field increases with increasing conductivity difference, and the electric field phase difference between the two ends of the line also increases, so the high-frequency component of the GIC decreases. Of course, the high-frequency component is very small in the GMD, so the negative coast effect only slightly influences the overall GIC.

V. CONCLUSION

In this paper, block and thin shell models for analyzing H-polarization are established. We then present the obtained geoelectric field distributions and the calculated relationships between the conductivity difference, f, and the geoelectric field distribution. A two-node model is established to study the influence of the lateral Earth conductivity variations on the GIC. The main results are as follows.

(1) In the horizontal direction perpendicular to the conductivity variations, the conductivity variations significantly influence the geoelectric field near the interface. The H-polarization increases the geoelectric field on the low-conductivity side and decreases the geoelectric field on the high-conductivity side. The increase in the geoelectric field is related to the variation of the vertical component of the telluric currents. In the block model, a k value of about 10 yields the maximum geoelectric field distortion, which is about 25% of the reference value.

(2) f only slightly affects the distortion amplitude of the geoelectric field with H-polarization, but it significantly influences the range. In the block model, the range of influence is 100 km, and the influence at low frequencies is much greater than that at high frequencies.

(3) The GIC calculation results show that when the conductivity difference is 5 times, the GIC increases by 10.53% compared to that without considering the H- polarization, while the actual conductivity difference is 10–4000 times and is concentrated on the surface. Therefore, the block model is insufficient to explain the GIC increases in coastal areas. In other words, the block model cannot be used to simulate the coast effect.

(4) The thin shell model is more suitable than the block model for coastal regions. The coast effect causes a maximum geoelectric field distortion of 1.5–6 times the reference value. With the same lateral conductivity difference, the distortion in the thin shell model is much larger than that in the block model. The surface lateral conductivity difference significantly influences the geoelectric field. Because of the phase difference between the geoelectric field near the interface and the reference value, the coast effect weakens the high-frequency component of the GIC located within 50 km of the coast and perpendicular to the coast.

(5) The influences of E- and H-polarization on geoelectric fields should be considered jointly. For example, for a transmission line located in a low-conductivity region adjacent to a high-conductivity area, the E-polarization weakens the geoelectric field component parallel to the interface, while the H-polarization increases the perpendicular component. If the transmission line parallel to the interface is long and sufficiently close to the interface, the influence of the proximity effect [21] on the GIC may be greater than that of the coast effect. Thus, the distance between the transmission line and interface and their relative orientation must be considered when determining the GIC. By doing so, the GIC calculation accuracy can be improved so that GIC high-risk areas can be identified more accurately.

In future work, current components of multiple frequencies can be superimposed to simulate space currents. Then, the effects of the conductivity, distance, and other parameters on the geoelectric field distortion and GIC can be calculated.

REFERENCES

[1] J. G. Kappernman and V. D. Albertson, "Bracing for the geomagnetic storms," *IEEE Spectr.*, vol. 27, no. 3, pp. 27–33, Mar. 1990.
[2] D. H. Boteler, R. J. Pirjola, and H. Nevanlinna, "The effects of geomagnetic disturbances on electrical systems at the Earth's surface," *Adv. Space Res.*, vol. 22, no. 1, pp. 17–27, 1998.
[3] R. Pirjola, "On currents induced in power transmission systems during geomagnetic variations," *IEEE Trans. Power App. Syst.*, vol. PAS-5, no. 10, pp. 42–43, Oct. 1985.
[4] J. T. Weaver, "The electromagnetic field within a discontinuous conductor with reference to geomagnetic micropulsations near a coastline," *Can. J. Phys.*, vol. 41, no. 3, pp. 484–495, 1963.
[5] W. D. Parkinson and F. W. Jones, "The geomagnetic coast effect," *Rev. Geophys.*, vol. 17, no. 8, pp. 1999–2015, 1979.
[6] D. H. Boteler and R. J. Pirjola, "Modelling geomagnetically induced currents produced by realistic and uniform electric fields," *IEEE Trans. Power Del.*, vol. 13, no. 4, pp. 1303–1308, Oct. 1998.
[7] G. Fischer, "Electromagnetic induction effects at an ocean coast," *Proc. IEEE*, vol. 67, no. 7, pp. 1050–1060, Jul. 1979.
[8] J. L. Gilbert, "Simplified techniques for treating the ocean–land interface for geomagnetically induced electric fields," *IEEE Trans. Electromagn. Compat.*, vol. 57, no. 4, pp. 688–692, Aug. 2015.
[9] F. Simpson and K. Bahr, *Practical Magnetotellurics*. Cambridge, U.K.: Cambridge Univ. Press, 2005.
[10] M. N. Berdichevsky and V. I. Dmitriev, *Models and Methods of Magnetotellurics*. Berlin, Germany: Springer, 2008.
[11] C. J. Weiss, "The two- and three-dimensional forward problems," in *The Magnetotelluric Method*, A. D. Chave and A. G. Jones, Eds. Cambridge, U.K.: Cambridge Univ. Press, 2012, ch. 7.
[12] J. L. Gilbert, "Modeling the effect of the ocean-land interface on induced electric fields during geomagnetic storms," *Space Weather*, vol. 3, no. 4, pp. 1–9, Apr. 2005.
[13] R. Horton, D. H. Boteler, T. J. Overbye, R. Pirjola, and R. C. Dugan, "A test case for the calculation of geomagnetically induced currents," *IEEE Trans. Power Del.*, vol. 27, no. 4, pp. 2368–2373, Oct. 2012.
[14] D. H. Boteler, "Geomagnetically induced currents: Present knowledge and future research," *IEEE Trans. Power Del.*, vol. 9, no. 1, pp. 50–58, Jan. 1994.
[15] D. S. Pipkins and S. N. Atluri, "Applications of the three dimensional finite element alternating method," *Finite Elem. Anal. Des.*, vol. 23, pp. 133–153, Nov. 1996.
[16] H. Y. Xiao and Y. Lei, *Geoelectric Tutorial*. Beijing, China: Geology Press, 2008, pp. 1–8.
[17] K. L. Shang, "Research and calculation of telluric current induced by magnetic storm," M.S. thesis, North China Electr. Power Univ., Beijing, China, 2012, pp. 28–30.
[18] Z. Z. Wang, B. Dong, and C. Liu, "Earth conductivity modelling technique for calculating geoelectric field during geomagnetic storms," *Sci. Tech. Eng.*, vol. 15, no. 13, pp. 72–76, 2015.
[19] Z. Wang, B. Dong, and C. Liu, "Three dimensional Earth conductivity structure modelling in north China and calculation of geoelectromagnetic fields during geomagnetic disturbances based on finite element method," *Trans. China Electrotech. Soc.*, vol. 30, no. 3, pp. 61–66, 2015.
[20] Z. Z. Wang and S. Q. Li, "Discussion of the electromagnetic interface conditions," *Trans. China Electrotech. Soc.*, vol. 28, no. 2, pp. 60–66, 2013.
[21] B. Dong, Z. Wang, L. G. Liu, L. P. Liu, and C. M. Liu, "The proximity effect on the induced geoelectric field at the interface of different conductivity structures with lateral variations during geomagnetic storms," (in Chinese), *Chin. J. Geophys.*, vol. 58, no. 1, pp. 238–246, 2015.

CHUNMING LIU was born in Hebei, China, in 1972. He received the B.S. degree in mechanical engineering from the Hebei University of Technology, China, in 1993, and the M.S. and Ph.D. degrees in electrical engineering from North China Electric Power University, in 2000 and 2009, respectively.

He has been a Professor with the North China Electric Power University. His current research interests include geomagnetically induced currents in power grids, including monitoring, modeling, and assessing the influence on the security of power systems.

XUAN WANG received the B.S. degree from the Hebei University of Technology, China, in 2014. She is currently pursuing the Ph.D. degree with the School of Electrical and Electronic Engineering, North China Electric Power University, Beijing, China.

Her research interests include the risk assessment of magnetic storm and prevention and control of power grid disaster.

SHUMING ZHANG received the M.S. degree from Northeast Electric Power University, China, in 2013. He is currently pursuing the Ph.D. degree with the School of Electrical and Electronic Engineering, North China Electric Power University, Beijing, China.

His research interests include the risk assessment of magnetic storm and prevention and control of power grid disaster.

CHUNZE XIE was born in Shandong, China, in 1996. He is currently pursuing the master's degree with North China Electric Power University. He is currently engaged in work related to the analysis of GIC.